Thin Solid Films 628 (2017) 13–21

Contents lists available at ScienceDirect

Thin Solid Films

journal homepage: www.elsevier.com/locate/tsf

Tailoring microstructure, mechanical and tribological properties of NiTi thin films by controlling in-situ annealing temperature

Soroush Momeni [a,*], Johannes Biskupek [b], Wolfgang Tillmann [a,*]

[a] Institute of Materials Engineering, Technical University of Dortmund, Leonhard-Euler-Str 2, 44227 Dortmund, Germany
[b] Electron Microscopy Department of Materials Science, University of Ulm, Albert-Einstein-Allee 11, 89081 Ulm, Germany

ARTICLE INFO

Article history:
Received 15 March 2016
Received in revised form 19 February 2017
Accepted 22 February 2017
Available online 24 February 2017

Keywords:
Nickel titanium
Shape memory alloy
Thin films
Wear
Adhesion
Microstructure
Tool steel

ABSTRACT

Magnetron sputtered near equiatomic NiTi thin films were deposited on Si (100) and hot work tool steel substrates. The deposited thin films were in-situ annealed at four different temperatures viz., 80 °C, 305 °C, 425 °C, and 525 °C. The effect of the in-situ annealing temperature on the microstructure of the film, the morphology, as well as mechanical and tribological properties was studied using X-ray diffraction, synchrotron diffraction, transmission electron microscopy, energy dispersive X-ray spectroscopy, ball-on-disc, scratch test, and three dimensional optical microscopy. The obtained results revealed how the variation of in-situ annealing temperature affects the crystallization, microstructure evolution, as well as mechanical and tribological properties of NiTi thin films.

1. Introduction

NiTi shape memory alloy (SMA) thin films with an equiatomic or near equiatomic composition ratio are an intermetallic compound of nickel and titanium. These thin films have long been classified as smart materials or ingredients of smart systems, due to their unique properties such as shape memory effect (SME) and superelasticity (SE). These unique properties are consequences of a reversible phase transformation capability from austenite to martensite phase and vice versa. Shape memory effect refers to the ability of NiTi to return to its original shape upon heating after an apparent plastic deformation. Superelasticity, however, is the ability of this alloy to return to its original shape upon unloading after being significantly strained. NiTi thin films must be well crystallized to demonstrate SME and SE. The crystallization of these thin films can be conducted by employing either a post-annealing treatment (annealing after deposition) or an in-situ annealing technique (annealing during deposition) [1].

Shape memory effect of NiTi thin films make them suitable materials for microelectromechanical systems (MEMS) [2] and thermomechanical data storage technology [3]. NiTi coatings are biocompatible [4] and can be used to deposit corrosion [5] and cavitation [6] resistant coating systems. The emerging thin film technology has further expanded the use of these coatings for medical devices [7]. For the last two decades, NiTi coatings were mainly investigated as reliable thin films within these broad fields of application. There are considerable number of high quality researches that investigates the deposition [8], processing optimization [9], microstructure [10], morphology [11], mechanical properties [12], phase transformation behavior [13], and crystallization [14] of these thin films. One issue which has not been properly investigated yet is the tribological performance of NiTi thin films, particularly their wear resistance and adhesion strength to the substrates.

Tribological performance of NiTi thin films is an important issue of concern. For example, the adhesion of surface micro-machined coatings to the underlying substrate can adversely affect efficiency and applicability of the thin films in MEMS [15]. Despite this importance, only few attempts have been made to analyze the wear and adhesion of NiTi thin films which were post-annealed after deposition [16,17]. The authors of this paper have recently reported the influence of the in-situ and post-annealing technique on the microstructure, phase transformation and tribological behavior of NiTi thin films [18]. It was found out that the in-situ annealed coatings have a remarkably better wear resistance and adhesion strength to the substrates when compared to post-annealed coatings. Due to the efficiency of in-situ annealing technique, it is worthwhile to further study the influence of in-situ annealing temperature on microstructure, mechanical and tribological performance of NiTi coatings.

* Corresponding authors.
E-mail addresses: soroush.momeni@tu-dortmund.de (S. Momeni), johannes.biskupek@uni-ulm.de (J. Biskupek), wolfgang.tillmann@udo.edu (W. Tillmann).

http://dx.doi.org/10.1016/j.tsf.2017.02.052
0040-6090/

This paper investigates the evolution of the microstructure of NiTi thin films upon varying the in-situ annealing temperature by using conventional as well as high-tech experimental techniques such as synchrotron X-ray diffraction and transmission electron microscopy (TEM). The main goal of this study, however, is to study the correlation between the evolution of the microstructure and tribological behavior of the deposited thin films. The obtained results present a processing route which is widely applicable to control the microstructure as well as the mechanical and tribological properties of NiTi thin films.

2. Experimental

The deposition of NiTi thin films was carried out on plasma nitrided hot work tool steel (X38CrMoV51) and Si (100) substrates by means of an industrial magnetron sputtering device (Cemecon MLsinox800, Germany). The plasma nitriding process of the tool steel substrates is explained in [19]. The coatings deposited onto the silicon wafers were used for four point probe resistivity measurements and transmission electron microscopy (TEM) images. The rest of the analyses were performed on the deposited coatings on the tool steel substrates. By comparing the results presented in [20], it was found that there is no significant changes in crystallographic phases and thicknesses of the NiTi coatings deposited under similar processing parameters on the tool steel and silicon wafer substrates. Two Ti-rich NiTi alloy targets (51.8 at% Ti-Ni) were employed to sputter NiTi thin films. In order to achieve an uniform film composition, the sample holder was rotated on a horizontal table during sputtering. The target to substrate distance was fixed at approximately 9.5 mm. NiTi thin films were annealed during sputtering (in-situ annealing or sputtering temperature) at four different temperatures of 525 °C, 425 °C, 305 °C, and 80 °C by adjusting the heating powers to 25,000 W, 10,000 W, 5000 W, and 0 W, respectively. Since the maximum applicable heating power was 10,000 W, an extra heating system, which supplied an additional 15,000 W of heating power, was installed inside the coating chamber. By employing this extra heating system, it was possible to reach the sputtering temperature of 525 °C. The deposition at the heating power of 0 W was performed without an intentional heating of the substrates. However, using the thermocouple, some substrate heating was detected around 80 °C during the deposition process. The temperature of the targets did not exceeded 60 °C because of the water circulating cooling system at the backside of the targets. Except the heating power, all sputtering parameters were kept constant during the deposition of NiTi thin films. These parameters are summarized in Table 1.

No post annealing process was conducted after the deposition of these films. The detailed description of the deposited thin films is presented in Table 2. The microstructure of the thin films was analyzed by employing X-ray diffraction using a Cu Kα (wavelength $\lambda = 0.15418$ nm) radiation and an incident angle of 9° (D8 Advance, BRUKER AXS, Germany). Further phase analysis of the deposited thin films was done by X-ray diffraction at the beamline BL9 of a synchrotron light source (DELTA, Germany). The incident photon energy was 27 keV (wavelength $\lambda = 0.4592$ Å), for the detection of the scattered intensity a MAR345 image plate detector was used. The beam size was 0.2×1.0 mm^2 (v × h) and the angle of incidence was set to 5°. The diffraction patterns were obtained from the MAR images using the FIT2D program package. Finally, the 2 theta scale of the diffraction patterns was converted to a wavelength of $\lambda = 1.5406$ Å. The thickness of the thin films was measured by means of a field emission scanning electron microscope (JEOL JSM-7001, Japan) and by analyzing a fractured cross-section of coated samples. The composition of the coatings was determined using energy-dispersive X-ray spectrometry (EDX) with an electron acceleration voltage of 20 kV and a beam current of 15 nA. All sampling was done by analyzing areas and not using point measurements to investigate the chemical compositions. Selected films were investigated to determine the crystal structure using transmissions electron microscopy (TEM) (Philips CM20, 200 kV operating voltage). Prior to TEM imaging, thin cross sectional samples were prepared by using mechanical grinding and polishing followed by low-angle Ar-ion etching to achieve electron transparency.

Table 2
Description of the specimens.

Sputtering time	In-situ annealing temperature	Composition Ni/Ti	Thickness
180 (min)	80 (°C)	50.55/49.45 (at%)	2.73 (μm)
180 (min)	305 (°C)	50.38/49.62 (at%)	3.43 (μm)
180 (min)	425 (°C)	50.66/49.34 (at%)	3.41 (μm)
180 (min)	525 (°C)	50.69/49.31 (at%)	2.97 (μm)

The nanoindentation tests were performed by a depth-controlled nanoindenter XP (MTS Nano instrument, USA) with a penetration depth of 10% of the coating thickness in order to minimize the effect of the substrate hardness on the measurement. During nanoindentation measurements, a Berkovic tip, made of a conductive diamond, was employed. Details of the nanoindentation method used in this research work was explained in [18]. Ball-on-disc tests were performed to examine the wear resistance of the coatings. During this test, a ball with a diameter of 6 mm, made of Al_2O_3, was employed as a counterpart for the coated rotating discs. The track radius and normal force were adjusted to 5 mm and 1 N for 7500 rotations. The cross-section areas of the wear tracks were measured at four different points by means of an Alicona 3D-analyzer (infinite focus) to calculate the average volume loss of the coating for each sample and the corresponding standard deviation. To evaluate the adhesion of the coatings, a micro-scratch test was performed using the single pass scratch mode with a diamond stylus topped as a conical. During the test, the force was linearly increased up to 100 N. Scratch tests were performed four times on each sample to calculate the arithmetic median and standard deviation.

3. Results

3.1. Crystalline structure of thin films

Due to the polymorphic crystallization of NiTi, an alloy of the same composition could contain different crystallographic structures and/or intermetallic phases. This leads to an overlapping of the diffraction pattern of different phases and makes it difficult to distinguish these phases by using conventional XRD techniques. In other words, the more similar the microstructures of two materials are the less different their diffraction patterns. The ability of the XRD technique to distinguish two similar crystalline/polymorphic structures mainly depends on the X-ray source as well as the diffractometer, detector, and calibration procedure applied. By using conventional XRD measurements, subtle phase analysis of polymorphs and intermetallics of polycrystalline materials can be dramatically hindered. As an alternative, the synchrotron radiation X-ray diffraction technique was introduced. Within this technique, X-rays are produced by a synchrotron facility which is at least 5 orders of magnitude more intense than the best X-ray laboratory source.

Fig. 1a and b show XRD profiles of in-situ annealed NiTi thin films at 80 °C and 305 °C between 2θ of 35° to 55°. Fig. 2c and d shows

Table 1
Processing parameters for deposition of NiTi SMA thin film interlayers.

Gas	Argon flow (ml/min)	Chamber pressure (mPa)	Substrate bias voltage (V)	Sputtering power (W)	Substrate rotation speed (rpm)
Ar	320	350	−0.075	1400	5

synchrotron XRD patterns of these coatings at 2θ of 35° to 55°. These XRD patterns illustrate nanocrystallization of coating materials at 80 °C and 305 °C. The synchrotron XRD patterns clearly reveals higher degree of nanocrystallization within in-situ annealed coating materials at 305 °C. This was figured out due to the peak splitting and appearance of a shoulder peak along the main peak in the synchrotron XRD pattern of in-situ annealed coating at 305 °C (Fig. 2d).

Fig. 2a and b indicate the XRD pattern of the in-situ annealed coatings at 425 °C and 525 °C between 2θ of 35° to 55° while Fig. 2c and d show synchrotron radiation X-ray diffractograms of these coatings at the same 2θ range. As it may be noted, the main diffraction pattern of in-situ annealed coatings at 2θ of 42.3° was split into two diffraction peaks demonstrating B2 austenite phase as well as R-phase. The higher peak intensity of R-phase reveals a higher volume fraction of this phase when compared to the austenite phase within the coating materials. By conducting synchrotron radiation X-ray diffraction analysis on the in-situ annealed coatings at 525 °C, a new diffraction pattern appeared between B2 austenite peak and R-phases. As reported earlier [18], this new peak is the major diffraction pattern of Ni_4Ti_3 precipitations, indexed as (122). It appeared due to the enlargement of the Ni_4Ti_3 precipitations. The largest volume fraction of the coating materials belong to the NiTi B2 austenite phase since its (110) diffraction peak intensity is the most pronounced diffraction pattern.

3.2. TEM

By performing X-ray diffraction analysis (XRD), it was found that in-situ annealed coatings at 80 °C are mainly amorphous while those in-situ annealed at 305 °C were semi-crystalline. The XRD analysis revealed that the in-situ annealed coatings at 425 °C and 525 °C are well-crystallized. Further examinations on the microstructure of the crystalline and semi-crystalline coatings were conducted by using transmission electron microscopy (TEM). According to previous studies, the crystallization of NiTi is polymorphic with a continuous nucleation and growth throughout the crystallization process [14]. Jiang et al. [21] reported earlier that the annealing at 300 °C leads to a nanocrystallization of NiTi shape memory alloys, subjected to sever plastic deformation. Their finding suggests the formation of nanocrystalline structures within the in-situ annealed NiTi coatings at 305 °C, as assumed in the XRD analysis (Fig. 1). This assumption was validated by performing TEM analysis. Fig. 3 shows TEM images of the in-situ annealed thin films at 305 °C, 425 °C, and 525 °C. TEM image of the in-situ annealed coating at 305 °C is gray and featureless, similar to previously reported results for amorphous NiTi thin films [1]. The inset diffraction patterns implies considerable amorphous volume fraction within the coating materials. Fig. 3b and c show TEM images of the in-situ annealed coatings at 425 °C and 525 °C, respectively. Their corresponding diffraction patterns revealed polycrystalline microstructure of these thin films.

The bright field and dark field TEM image of in-situ annealed coatings at 305 °C are shown in Fig. 4. As can be seen, high magnification dark-field images clearly reveals nanocrystalline structure of the films containing grains with sizes in the range of 10 nm to 20 nm (Fig. 4d). It was found that all combinations of different elements cannot inherently form alloys films with a nanocrystalline structure. In fact, four possible routes were introduced to form nanocrystalline or X-ray amorphous films: (i) fast cooling of the alloy from a liquid state; (ii) addition of metalloid such as Si, B, C, and N to a host one–element material, for example TiC; (iii) selection of an appropriate amount of both elements in the alloy, for example Ag-Ni and Al-Ti; (iv) Fabrication of a nitride of the alloy by addition of a certain amount of nitrogen to the alloy, for example TiAlN and CrAlN [22]. The result of current study revealed that selection of an equiatomic composition ratio in NiTi alloys results in formation of nanocrystalline films. This, in turn, corresponds with the third processing route mentioned above.

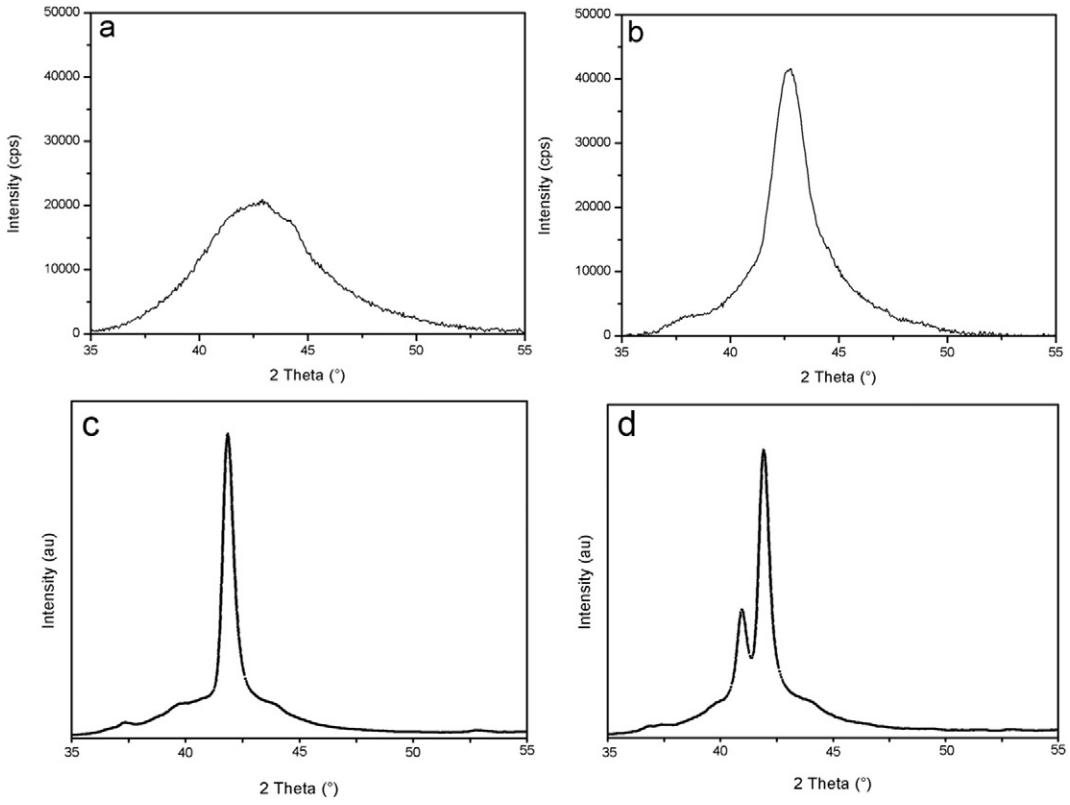

Fig. 1. (a) conventional XRD patterns of in-situ annealed NiTi thin films at 80 °C (b) conventional XRD pattern of in-situ annealed coating at 305 °C (c) synchrotron radiation XRD pattern of in-situ annealed NiTi thin films at 80 °C (d) synchrotron radiation XRD pattern of in-situ annealed NiTi thin films at 305 °C.

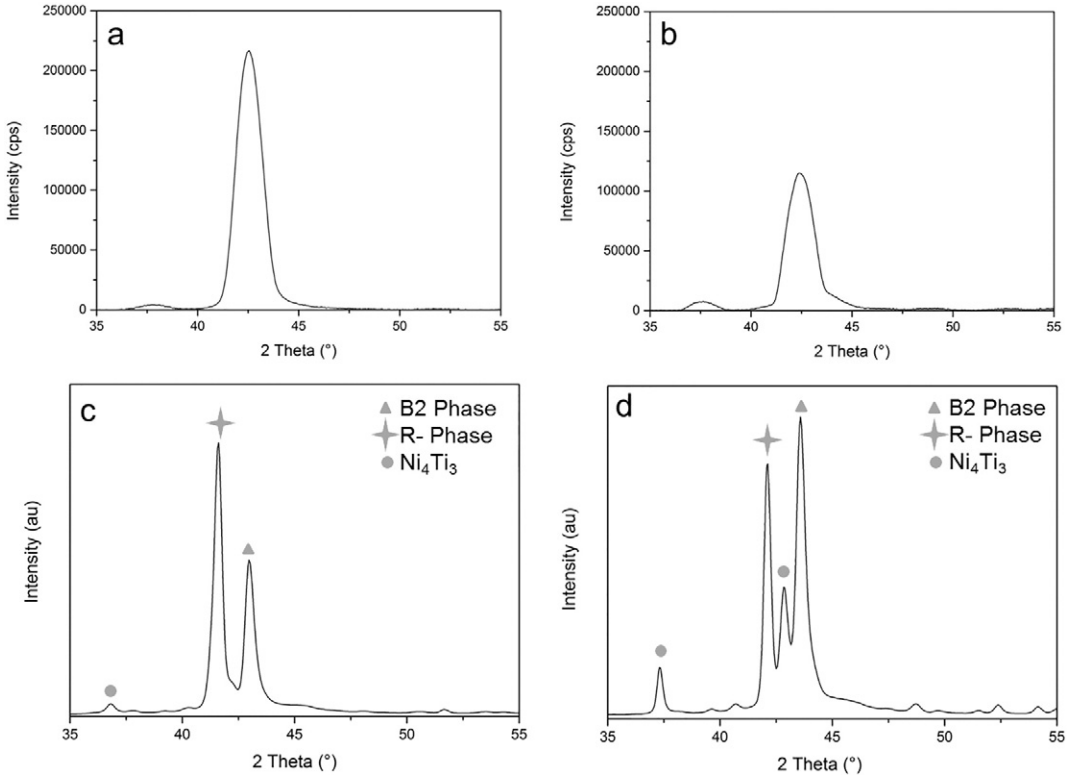

Fig. 2. (a) Conventional XRD patterns of in-situ annealed NiTi thin films at 425 °C (b) conventional XRD pattern of in-situ annealed coating at 525 °C (c) synchrotron radiation XRD pattern of in-situ annealed NiTi thin films at 425 °C (d) synchrotron radiation XRD pattern of in-situ annealed NiTi thin films at 525 °C.

Bright field and corresponding dark field TEM images of in-situ annealed coatings at 425 °C are shown in Fig. 5. TEM analysis revealed the growth of single grains with the length up to 3 μm through whole of the film. In the case of thin films, one would expect a stagnation of normal grain growth when the mean grain dimensions approach the order of the layer thickness [23]. An et al., [24] used Monte Carlo simulation to present a three stage model of the grain size evolution in thin films by taking into account the thickness effect. In stage 1, normal grain growth proceeds without any obstacle as the average grain size is considerably smaller than the film thickness. Grain growth slows

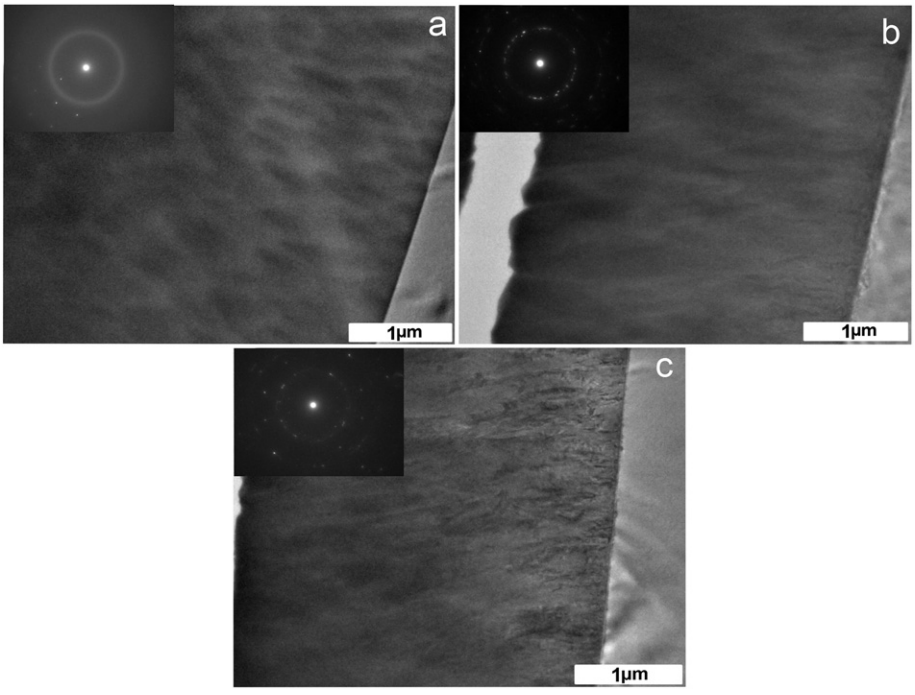

Fig. 3. Cross section TEM images of the in-situ annealed NiTi thin films at (a) 305 °C, (b) 425 °C and (c) 525 °C. The top-left insets show selected area electron diffraction revealing the amorphous structure in (a) as well as polycrystalline structure in (b) and (c).

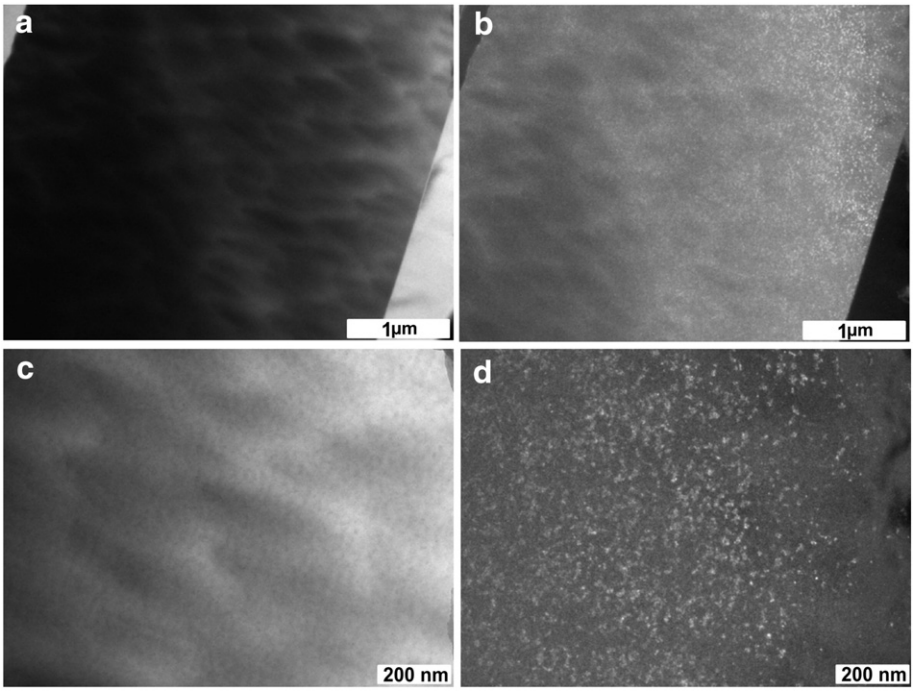

Fig. 4. Bright and dark field TEM micrographs of the in-situ annealed NiTi thin films at 305 °C.

down with the formation of columnar grains in stage 2. These columnar grains extend through the entire film and intersect the surface. All grains extend through the film and growth almost stops in stage 3. In spite of this, one could expect the straitening of grain boundaries and the consumption of small grains by adjacent larger grains (via Ostwald ripening) in stage 3. Stage 1 of this model could correspond to in-situ annealing of NiTi coatings at 305 °C in which nano grains were formed. In-situ annealing of NiTi coatings at 425 °C could be attributed to stage 2 of this model since the grain size of this coatings is comparable to the film thickness and also the grains intersects the surface.

The increment of the in-situ annealing temperature resulted in further densification and reduction of the film thickness. The nano-textured structure of the in-situ annealed coatings at 525 °C can be obviously observed in Fig. 6. The bright field and corresponding dark field TEM images of these coatings are shown in Fig. 7. The in-situ annealed coatings at 525 °C possess the grains with the length of 1–2 μm and the width of 0.2–0.5 μm. The grains are considerably shorter than those observed in the in-situ annealed coatings at 425 °C. This difference in grain size is a direct consequence of an inherent competition between nucleation and growth during

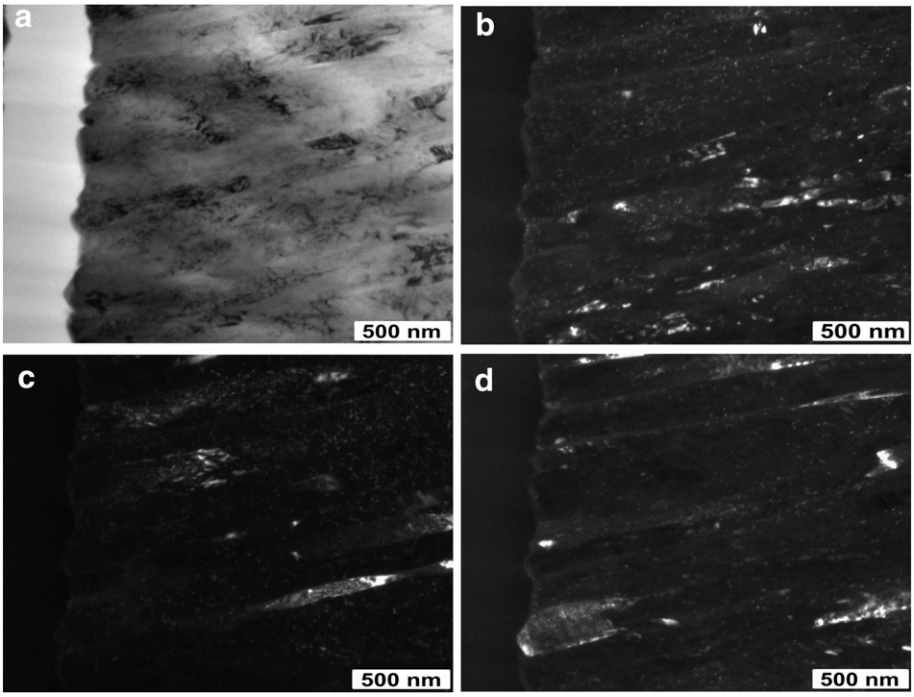

Fig. 5. Bright and dark field TEM micrographs of the in-situ annealed NiTi thin films at 425 °C.

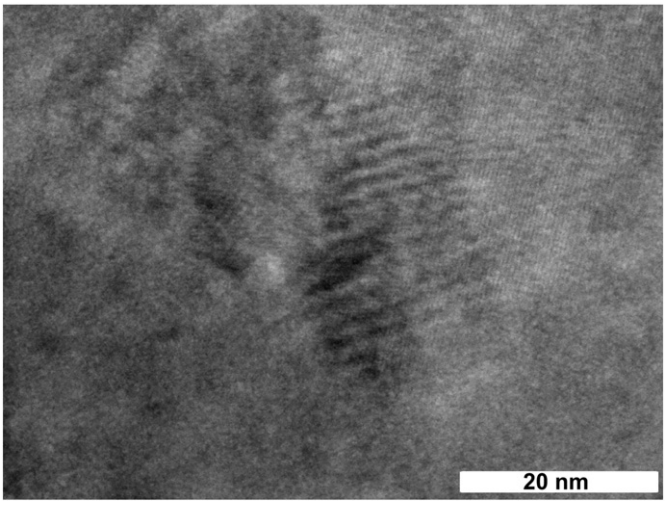

Fig. 6. TEM image of NiTi grains within the in-situ annealed coatings at 525 °C.

crystallization. Generally speaking, the crystallization process is driven by the difference in the chemical potential between the amorphous and crystalline phase. The transformation from the crystalline to amorphous phase breaks into two stages: nucleation and growth of grains. The minimization of the total grain boundary area is the driving force for the grain growth in the polycrystalline material [25]. Reimerz et al., [26] performed in-situ TEM observation during crystallization of amorphous NiTi coatings. According to their finding, both nucleation and growth increase with temperature while nucleation is more strongly dependent on temperature. Thus, at low temperature, a large grained microstructure should be formed due to the low number of crystals. Furthermore, based on the obtained results regarding the thickness of the in-situ annealed coatings, it can be assumed that the film thickness can be influenced by crystal growth velocity rather than nucleation rate.

3.3. Phase transformation

The authors of the current study investigated phase transformation of near equiatomic NiTi coatings which were in-situ annealed at 425 °C and 525 °C [18,20]. According to differential scanning calorimetry (DSC) and 4-point probe resistivity measurements, in-situ annealing of near equiatomic NiTi coatings above 425 °C results in the formation of the reversible martensitic phase transformation within the coating materials. Fig. 8 shows the temperature dependence of the electrical resistance (ER) for in-situ annealed NiTi thin films at 80 °C and 305 °C. The resistance versus temperature (RT) plots these thin films show no phase transformation within the coating materials. The RT plots display an unusual behavior in which the resistivity decreases during heating and it increases during cooling process. Such a semiconductor-like behavior was earlier observed by [27] for RT plot of Ni_XTi_{1-X} (X = 52.7) thin film post annealed at 600 for 30 min.

3.4. Nanoindentation

Fig. 9 illustrates the measured hardness and Young's modulus of the deposited coatings by employing nanoindentation. The hardness and Young's modulus of the in-situ annealed thin films at 80 °C and 305 °C are quite close to each other, probably due to their mostly amorphous microstructure. Increasing the in-situ annealing temperature to 425 °C results in 40% decreases in the values of hardness and Young's modulus of the NiTi thin films. The reduction in hardness and Young's modulus is due to the crystalline microstructure of in-situ annealed thin films at 425 °C. In general, crystalline NiTi thin films are softer than as-deposited ones. The XRD analysis revealed that the in-situ annealed thin films at 80 °C and 305 °C are mostly amorphous while the in-situ annealed thin films at 425° are well crystallized and contain B2 austenite as well as R phase. The inherent superelasticity of austenite phase can lower the hardness as a consequence of the reversible isothermal phase transformation from austenite to martensite upon loading and unloading [28]. Moreover, R phase is also capable of presenting reversible phase transformation behavior (i.e., superelasticity) but in a smaller

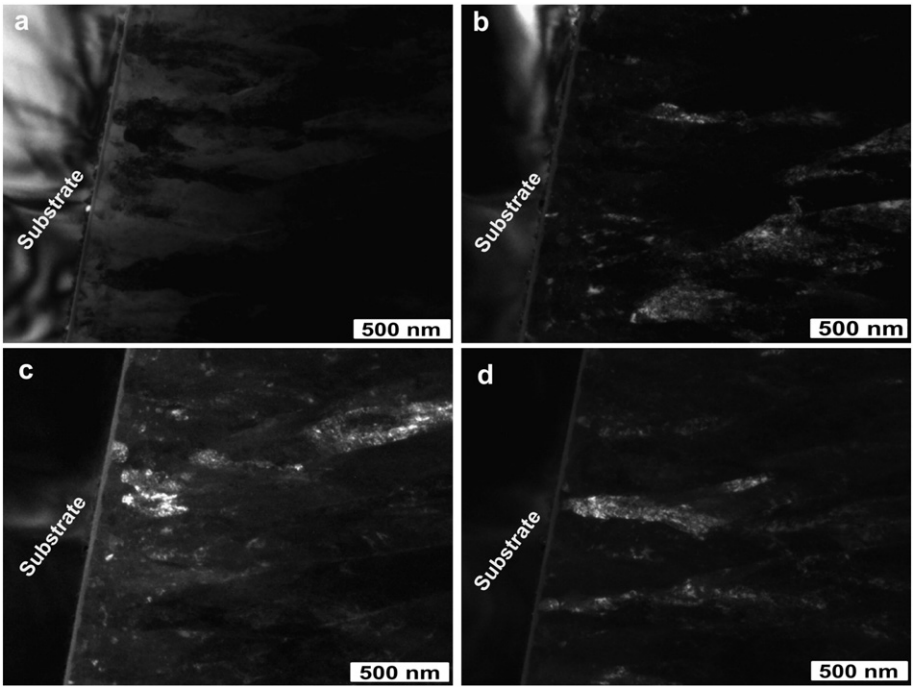

Fig. 7. Bright and dark field TEM micrographs of the in-situ annealed NiTi thin films at 525 °C.

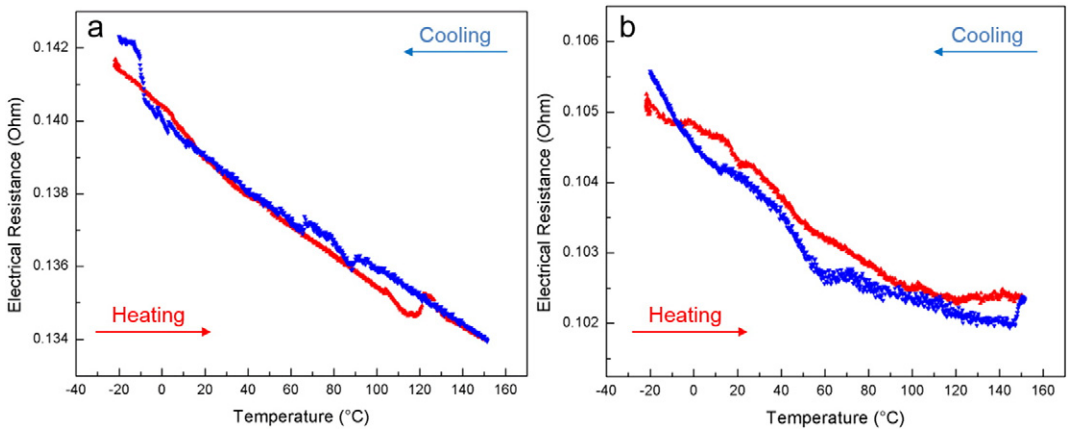

Fig. 8. Resistance as a function of measurements temperature for near equiatomic NiTi films in-situ annealed at (a) 80 °C and (b) 305 °C.

magnitude [29]. This, in fact, can also participate in lowering of the hardness during Nanoindentation test.

While the in-situ annealing temperature was raised from 425 °C to 525 °C, NiTi B2 austenite coating materials were further crystallized. In this step, by raising the in-situ annealing temperature, hardness and Young's modulus values were up to 30% increased. The increment in hardness and Young's modulus can be explained by considering two postulations.

The first postulation is based on the link between the evolution of the crystallization process and mechanical properties of the thin films. The XRD patterns of in-situ annealed thin films at 425 °C revealed appropriate crystallization of the coating materials. Since the crystallization temperature of sputtered NiTi thin films is about 550 °C, it can be concluded that the in-situ annealed thin films at 425 °C were not completely crystallized and contain some amorphous regions. Amorphous alloys can be regarded as frozen melt structures without any long-range order in three dimensions. By annealing treatments around glass transition temperature, but below crystallization temperature, an atomic-level rearrangement occurs. This phenomenon is termed structural relaxation in which short-range orders evolve from amorphous coatings [10]. Structural relaxation results in densification of the films, reduction in thickness of the films as well as increment of hardness and Young's modulus [30]. Thus, in the current study, it can be assumed that elevating the in-situ annealing temperature to 525 °C leads to the structural relaxation within the amorphous volume fraction of the coatings. The decrease in the thickness of the thin films was shown in Section 3.2 and discussed in [20].

According to the second postulation, the increase in hardness and Young's modulus values is due to the grain size reduction. The nucleation and growth rates increase by raising temperature during crystallization of NiTi thin films. The nucleation, however, is more strongly dependent on temperature. The stronger temperature dependency of nucleation process leads to formation of small-grained microstructure at high temperatures, where the nucleation rate is high [26]. At low temperatures, due to the small number of crystals, a large-grained microstructure appears. The smaller grain size of the in-situ annealed thin films at 525 °C results in creation of a larger number of grain boundaries. Expansion of the grain boundaries strengthens the coating materials and increases the hardness values. The increment of hardness was collocated with the increasing of Young's modulus values.

3.5. Tribology

The tribological properties of thin film coatings are strongly influenced by changing in-situ annealing temperature (sputtering temperature). Fig. 10 shows the obtained numerical values for the critical loads of the deposited thin films along with their specific wear rates. The in-situ annealed coatings deposited at 80 °C have the smallest critical load which shows these coatings have the poorest adhesion strength to the substrates. Due to the brittleness of the amorphous microstructure, these coatings are unable to resist against loading of the diamond stylus and therefore, they were easily detached from the substrates. As reported by D.M. Mattox [31], the inter-diffusion between sputtered atoms and substrate materials is an important factor affecting the coating to substrate adhesion. It is also known that the diffusion process of the atoms is directly proportional to the temperature [32]. In-situ annealing at a low temperature of 80 °C leads to small degree of inter-diffusion between sputtered atoms and the substrate materials. Such a weak inter-diffusion results in a poor coating-to-substrate adhesion. In spite of the fact that the in-situ annealed thin films at 305 °C are mostly amorphous, their critical load is larger than that of the crystallized coatings at in-situ annealing temperature of 425 °C. The contributing factor for this phenomenon is the formation of nanocrystalline NiTi in the amorphous matrix. The XRD measurement and TEM analysis revealed formation of the nanocrystalline structure within in-situ annealed NiTi coatings at 305 °C. As a result, it can be assumed that the in-situ annealing of NiTi coatings at 305 °C created a unique dual-phase composite coating of the nanocrystalline NiTi embedded in the brittle NiTi amorphous matrix. Nanostructured soft/hard dual-phase composites are capable to exhibit high strength and large ductility simultaneously.

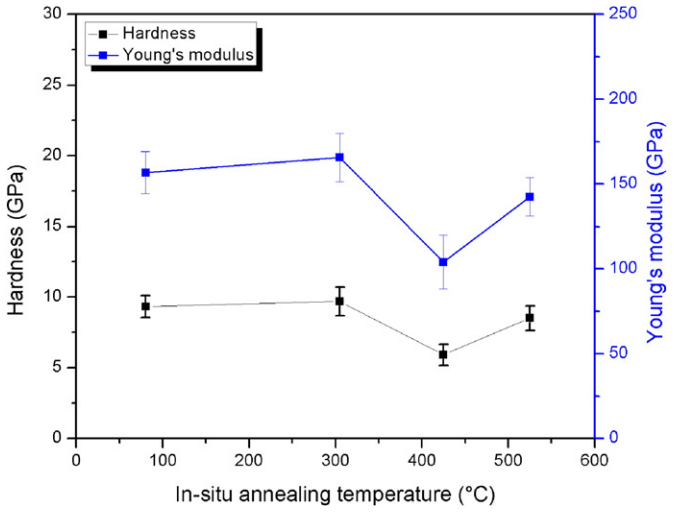

Fig. 9. Hardness and Young's modulus values obtained from nanoindentation tests on in-situ annealed NiTi coatings.

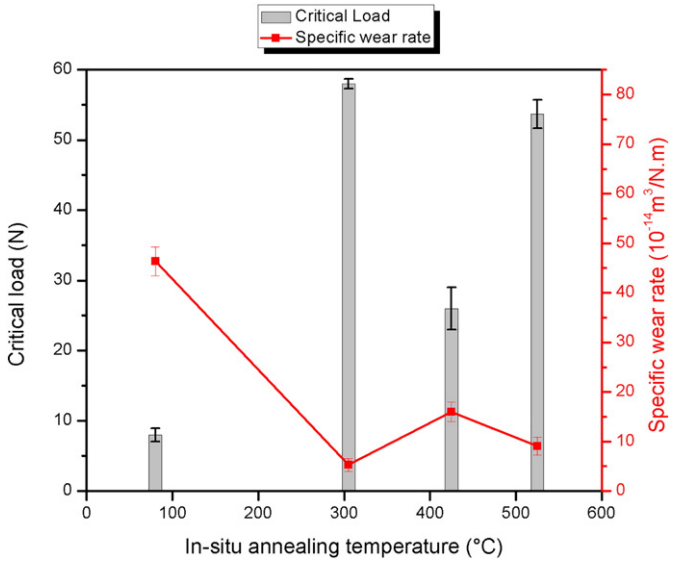

Fig. 10. Specific wear rate and critical loads of in-situ annealed NiTi coatings.

This is due to the fact that the interaction between the soft and hard components during deformation results in enhancement of mechanical properties [33].

The in-situ annealed coatings at 425 °C present a weaker coating-to-substrate adhesion. It could be attributed to its mostly crystallized microstructure with B2 superelastic austenite as well as R phase. This phases have a rubber-like behavior due to their superelasticity and thus, cannot properly sustain against the progressive load of the diamond stylus. By increasing the in-situ annealing temperature to 525 °C, the adhesion of the coatings to the substrates was effectively increased. The reason for this increment, as it was discussed in Section 3.4, is development of the microstructure of NiTi coatings which enhanced their strength. Another contributing factor might be the increment in inter-diffusion of sputtered atoms and substrate materials at a higher temperature of 525 °C.

As indicated in Fig. 10, the in-situ annealed coatings at 80 °C have the largest specific wear rate. It was found that the in-situ annealed thin films at low temperature of 80 °C are fully mainly with brittle behavior and have a weak adhesion to the substrates. These all result in poor wear resistance of these thin films during the sliding wear test. As discussed in the previous sections, in-situ annealing treatment at 305 °C leads to the formation of metallic glasses nanocomposite coatings in which nanocrystalline NiTi were distributed in an amorphous matrix. These nanocrystalline constituents in the amorphous matrix allow plastic strains to be accommodated and consequently, could benefit the wear resistance behavior. The lack of grain boundary in this coating can be of significant benefit along with high yield of strength. Such a coating system has a high potential for certain mechanical and tribological applications. This is due to the capability of amorphous matrix/crystalline-fibre composite materials to delocalize shear band formation [34].

While raising the in-situ annealing temperature from 305 °C to 425 °C, the specific wear rate of the NiTi coatings increases. In this step, increasing the in-situ annealing temperature leads to further crystallization of NiTi coatings and disappearance of metallic glasses nanocomposite microstructure. Therefore, there is no enhancing effect of nanocrystalline NiTi for improving mechanical and tribological enhancement of the coatings.

The increment of in-situ annealing temperature from 425 °C to 525 °C, however, resulted in decrement of the specific wear rate. There are two reasons for the improvement of the wear resistance of the coatings in this step. The first one is due to the structural relaxation during full crystallization process of NiTi coatings which could effectively improve their mechanical and subsequently, tribological performance. The second reason is the enlargement (in quantity and size) of Ni_4Ti_3 precipitation by increasing the in-situ annealing temperature, as discussed in Section 3.1. These metastable precipitations are known for strengthening NiTi austenite phase and reducing plastic deformation during load cycling [35]. Arciniegas et al. [36] reported an improvement in wear resistance of NiTi bulk alloys due to the presence of the semi-coherent Ni_4Ti_3 precipitations in B2 austenite phase. Their finding in wear analysis of NiTi bulk alloys corresponds interestingly with the obtained result of the current research work in wear analysis of NiTi thin films.

4. Conclusion

This paper investigated the effect of in-situ annealing temperature (sputtering temperature or substrate temperature) on microstructure, morphology, phase transformation, mechanical and tribological properties of NiTi thin films. It was found that mechanical and tribological behaviors of NiTi thin films can be tailored by adjusting in-situ annealing temperature.

According to XRD analyses, the films deposited at 80 °C and 305 °C are mainly amorphous. TEM analysis revealed that NiTi nano grains (10–20 nm) were formed within in-situ annealed coatings at 305 °C. Deposition at a sputtering temperature above 425 °C leads to the formation of well-crystallized NiTi thin films as well as Ni_4Ti_3 precipitations. Raising the in-situ annealing temperature from 425 °C to 525 °C resulted in enlargement and further crystallization of Ni_4Ti_3 precipitations. This, however, resulted in formation of smaller crystallized NiTi grains.

The Nanoindentation analysis revealed that the hardness and Young's modulus of the in-situ annealed coatings at 80 °C and 305 °C are quite close to each other, perhaps due to their dominantly amorphous microstructure. NiTi coatings in-situ annealed at 425 °C possesses lower hardness and Young's modulus when compared to the in-situ annealed coatings at 80 °C and 305 °C. The reason for this is the formation of NiTi B2 austenite phase which can lower the hardness due to the superelasticity of NiTi austenite phase. While the in-situ annealing temperature increased from 425 °C to 525 °C, the hardness and Young's modulus increased again. The reason for this might be attributed to the structure relaxation of remained amorphous phases and/or formation of smaller grains at higher in-situ annealing temperature.

The in-situ annealed coatings at 80 °C presented a poor wear resistance behavior due to its mainly amorphous microstructure. Despite the dominantly amorphous microstructure of in-situ annealed coatings at 305 °C, they possess an excellent wear resistance capability. This is due to the formation and distribution of nano grains of NiTi in the amorphous matrix which created a nanostructured soft/hard dual-phase composite with an enhanced wear resistance behavior. Further increasing of the in-situ annealing temperature to 425 °C resulted in degradation of the wear resistance behavior, perhaps due to the removal of the nanostructured composite phase. By raising the in-situ annealing temperature to 525 °C, the wear resistance of the coatings enhanced again, probably due to the structural relaxation and/or enlargement (in quantity and size) of Ni_4Ti_3 precipitates.

The adhesion strength of the in-situ annealed coatings showed a similar trend to their wear resistance capability. In-situ annealed coatings at 80 °C demonstrated a poor coating-to-substrate adhesion. Raising the in-situ annealing temperature to 305 °C resulted in significant enhancement of the coating-to-substrate adhesion due to the formation of nanostructured composite phase. In-situ annealing of the coatings at 425 °C resulted in degradation in adhesion strength of the coatings due to removal of the nanocomposite phase. Increasing the in-situ annealing temperature to 525 °C improved the coating to substrate adhesion due to a higher inter-diffusion of sputtered atoms in the substrate at higher temperature and/or microstructural enhancement.

Acknowledgement

The authors thank Dr. Christian Sternemann from the DELTA machine group and Leif Hagen from the Institute of Materials Engineering at TU Dortmund University for organizing and performing synchrotron X-ray diffraction measurements. The authors thank Dr. Sigurd Thienhaus for conducting 4-point probe resistivity measurements at Ruhr University of Bochum (RUB) in Germany.

References

[1] G. Satoh, A. Birnbaum, Y.L. Yao, Annealing effect on the shape memory properties of amorphous NiTi thin films, J. Manuf. Sci. Eng. 132 (5) (2010) 051004, http://dx.doi.org/10.1115/1.4002189.
[2] N. Choudhary, D.K. Kharat, D. Kaur, Surface modification of NiTi/PZT heterostructure thin films using various protective layers for potential MEMS applications, Surf. Coat. Technol. 206 (2011) (1735–1743).
[3] Wendy C. Crone, Gordon A. Shaw, Applying NiTi shape-memory thin films to thermomechanical data storage technology, MRS Proc. 855 (W1) (2004) 7, http://dx.doi.org/10.1557/PROC-855-W1.7.
[4] K. Loger, R. Lima de Miranda, A. Engel, M. Marczynski-Bühlow, G. Lutter, E. Quandt, Fabrication and evaluation of nitinol thin film heart valves, Cardiovasc. Eng. Technol. 5 (4) (2014) 308–316.
[5] M.R. Gorji, S. Sanjabi, Corrosion behavior of ion implanted NiTi shape memory alloy thin films, Mater. Lett. 73 (2012) 179–182.
[6] S. Momeni, W. Tillmann, M. Pohl, Composite cavitation resistant PVD coatings based on NiTi thin films, Mater. Des. 110 (2016) 830–838.
[7] Y. Chun, D.S. Levi, K.P. Mohanchandra, G.P. Carman, Superhydrophilic surface treatment for thin film NiTi vascular applications, Mater. Sci. Eng. C 29 (8) (2009) 2436–2441.
[8] K. Ho, K.K. Mohanchandra, G.P. Garmen, Examination of the sputtering profile of NiTi under target heating conditions, Thin Solid Films 413 (1–2) (2002).
[9] H.D. Gu, K.M. Leung, C.Y. Chung, L. You, X.D. Han, K.S. Chan, J.K.L. Lai, Pulsed laser deposition of NiTi shape memory alloy thin films with optimum parameters, Thin Solid Films 330 (1998) 196–201.
[10] X. Huang, A.G. Ramirez, Structural relaxation and crystallization of NiTi thin film metallic glasses, Appl. Phys. Lett. 95 (2009) 121911.
[11] L. Zhang, C. Xie, J. Wu, Effect of annealing temperature on surface morphology and mechanical properties of sputter-deposited Ti–Ni films, Alloys Compd. 427 (2007) 238–243.
[12] A. Kumar, D. Singh, D. Kaur, Grain size effect on structural, electrical and mechanical properties of NiTi thin films deposited by magnetron co-sputtering, vol. 203, Issue 12, 2009 March 15, pp. 1596–1603, http://dx.doi.org/10.1016/j.surfcoat.2008.12.005.
[13] Huang Xu, J. San Juan, A.G. Ramirez, Evolution of phase transformation behavior and mechanical properties with crystallization in NiTi thin films, Scr. Mater. 63 (1) (2010 July) 16–19.
[14] X. Wang, M. Rein, J.J. Viassak, Crystallization kinetics of amorphous equiatomic NiTi thin films: effect of film thickness, J. Appl. Phys. 103 (2008) 023501.
[15] W. Robert Ashurst, C. Carraro, R. Maboudian, Vapor phase anti-stiction coatings for MEMS, IEEE Trans. Device Mater. Reliab. 3 (4) (2003) 173–178.
[16] T. Abubakar, M. Rahman, J. Stokes, Effect of annealing treatment on the wear properties of Ni rich NiTi alloy coatings, Adv. Mater. Res. 686 (2013) 192–200, http://dx.doi.org/10.4028/www.scientific.net/AMR.686.192.
[17] K.L. Ng, Q.P. Sun, M. Tomozawa, S. Miyazak, Wear behavior of NiTi thin film at microscale, Int. J. Mod. Phys. B 24 (1 & 2) (2010) 85–93, http://dx.doi.org/10.1142/S0217979210064010.
[18] W. Tillmann, S. Momeni, Influence of in-situ and postannealing technique on tribological performance of NiTi SMA thin films, Surf. Coat. Technol. 276 (2015) 286–295.
[19] W. Tillmann, S. Momeni, F. Hoffmann, A study of mechanical and tribological properties of self-lubricating TiAlVN coatings at elevated temperatures, Tribol. Int. 66 (2013) 324–329.
[20] W. Tillmann, S. Momeni, In-situ annealing of NiTi thin films at different temperatures, Sensors Actuators A 221 (1) (2015) 9–14.
[21] S. Jiang, Y. Zhang, L. Zhao, Y. Zheng, Influence of annealing on NiTi shape memory alloy subjected to sever plastic deformation, Intermetallics 32 (2013) 344–351.
[22] A. Cavaleiro, J.T.M. De Hosson, Nanostructured coatings, Springer, 2006 407–463.
[23] S. Heiroth, R. Frison, J.L.M. Rupp, T. Lippert, E.J.B. Meier, E.M. Gubler, et al., Crystallization and grain growth characteristics of yttria-stabilized zirconia thin films grown by pulsed laser deposition, Solid State Ionics 191 (2011) 12–23.
[24] Z.A. An, H. Ding, Q.P. Meng, Y.H. Rong, Kinetic equation of the effect of thickness on grain growth in nanocrystalline films, Scr. Mater. 61 (2009) 1012–1015.
[25] W.D. Callister, D.G. Rethwisch, Materials Science and Engineering: an Introduction, eighth ed. John Wiley and Sons, 2009 December 30.
[26] A.G. Ramirez, H. Ni, H.J. Lee, Crystallization of amorphous sputtered NiTi thin films, Mater. Sci. Eng. A 438–440 (2006) 703–709.
[27] N.L.H. Odum, The Characterization of Thin Film NiTi Shape Memory Alloy, Auburn University, 2010 PhD thesis.
[28] W. Tillmann, S. Momeni, Comparison of NiTi thin films sputtered from separate elemental targets and Ti-rich alloy targets, J. Mater. Process. Technol. 220 (2015) 184–190.
[29] T.W. Duering, K. Bhattacharya, The influence of the R-phase on the superelastic behavior of NiTi, Shape Mem. Superelast. 1 (2) (2015) 153–161, http://dx.doi.org/10.1007/s40830-015-0013-4.
[30] Z. Han, G. Li, J. Tian, M. Gu, Microstructure and mechanical properties of boron carbide thin films, Mater. Lett. 57 (2002) 899–903.
[31] D.M. Mattox, Particle bombardment effects on thin-film deposition: a review, J. Vac. Sci. Technol. A 7 (1989) 1105.
[32] F.W. Bach, A. Laarmann, T. Wenz, Modern Surface Technology, 13, Wiley-VCH, 2004.
[33] A. Leyland, A. Matthews, Design criteria for wear-resistant nanostructured and glassy-metal coatings, Surf. Coat. Technol. 177–178 (2004) 317–324.
[34] W.L. Johnson, Bulk glass-forming metallic alloys: science and technology, MRS Bull. 24 (10) (1999) 42.
[35] N. Zhou, C. Shen, M.F.-X. Wagner, G. Eggeler, M.J. Mills, Y. Wang, Effect of Ni4Ti3 precipitation on martenistic transformation in Ni-Ti, Acta Mater. 58 (2010) 6685–6694.
[36] M. Arciniegas, J. Casals, J.M. Manero, J. Peña, F.J. Gil, Nanoscale indentation behavior of pseudo-elastic Ti–Ni thin films, J. Alloys Compd. 465 (2008) 491–496.